IEEE Photonics Journal
An IEEE Photonics Society Publication

Open Access

Novel Method for Improving the Capacity of Optical MIMO System Using MGDM

Volume 6, Number 6, December 2014

F. Baklouti
I. Dayoub, Senior Member, IEEE
S. Haxha, Senior Member, IEEE
R. Attia
A. Aggoun

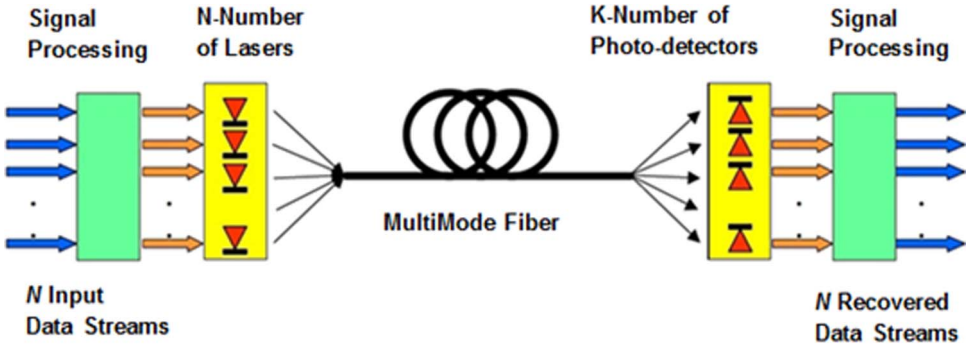

Optical Multiple-Input-Multiple-Output Multiplexing of Parallel Communication Multichannels over a Single MultiMode Fiber Network

DOI: 10.1109/JPHOT.2014.2363444
1943-0655

IEEE photonics SOCIETY

IEEE

Novel Method for Improving the Capacity of Optical MIMO System Using MGDM

F. Baklouti,[2] I. Dayoub,[3] *Senior Member, IEEE*, S. Haxha,[1,4] *Senior Member, IEEE*, R. Attia,[2] and A. Aggoun[1]

[1]Department of Computer Science and Technology, University of Bedfordshire, Luton LU1 3JU, U.K.
[2]Polytechnic School of Tunisia (EPT), 2078 Tunis, Tunisia
[3]Département d'Opto Acousto et d'Electronique de l'Institut d'Electronique de Microélectronique et de Nanotechnologie (IEMN DOAE), Université de Valenciennes, 59313 Valenciennes, France
[4]School of Engineering and Digital Arts, University of Kent, Canterbury CT2 7NJ, U.K.

DOI: 10.1109/JPHOT.2014.2363444

Manuscript received July 7, 2014; revised October 2, 2014; accepted October 11, 2014. Date of publication October 16, 2014; date of current version October 27, 2014. Corresponding author: S. Haxha (e-mail: shyqyri.haxha@beds.ac.uk).

Abstract: In current local area networks, multimode fibers (MMFs), primarily graded index (GI) MMFs, are the main types of fibers employed for data communications. Due to their enormous bandwidth, it is considered that they are the main channel medium that can offer broadband multiservices using optical multiplexing techniques. Amongst these, mode group diversity multiplexing (MGDM) has been proposed as a way to integrate various services over an MMF network by exciting different groups of modes that can be used as independent and parallel communication channels. In this paper, we study optical multiple-input–multiple-output (O-MIMO) systems using MGDM techniques while also optimizing the launching conditions of light at the fiber inputs and the spot size, radial offset, angular offset, wavelength, and the radii of the segment areas of the detectors. We propose a new approach based on the optimization of launching and detection conditions in order to increase the capacity of an O-MIMO link using the MGDM technique. We propose a (3×3) O-MIMO system, where our simulation results show significant improvement in GI MMFs' capacity compared with existing O-MIMO systems.

Index Terms: Optical communication systems, optical MIMO, MGDM, channel capacity, spatial emission.

1. Introduction

The use of optical fiber is of great interest in developing extensive, high-speed networking infrastructures. Optical fiber provides many advantages over traditional copper cables and wireless links [1]. Among these advantages are high security, low electromagnetic interference, extremely low loss, very high bandwidths, and highly manageable cabling. In short range optical networks, where the length of the optical fibers does not exceed a few kilometers, MMFs have been primarily used. A good reason for this is that the size of their core is much larger than the size of the core of single-mode fibers (SMFs). Therefore, handling of MMFs is easier than of SMFs, since there is more tolerance in the required alignment for the coupling of light in and out of the MMF, as well as for splicing MMFs.

While the plurality of modes in MMF eases requirement on optoelectronic components and fiber alignment, it also leads to distortion of the transmitted signal. The guided modes of MMF

exhibit unique group velocity. In stepped-Index Multimode Fiber (SI-MMF), modes of increasing order (i.e., complexity in transverse mode profile) also propagates along an increased path length. In a homogenous medium, signal transmitted along more the High-Ordered Modes (HOM) will have a longer effective path length and will arrive at the fiber output significantly later than signal in Low-Ordered Modes (LOM). This intermodal dispersion, or Differential Modal Delay (DMD), can cause severe Inter-Symbol Interference (ISI). The core of GI-MMF, however, is designed to minimize this DMD among modes. Besides exhibiting a shorter path length than HOM, LOM are confined to smaller regions, near the center of the fiber core; as a result, LOM experience a higher refractive index. Due to their large core diameters compared to the SMF, GI-MMFs offer major advantages in installation, handling and in capacity benefits. They enable necessary bandwidth for short length applications such as e.g., local area networks, data centers, and radio over fiber, etc. As a result, this study is devoted to GI-MMFs system performance.

Currently, we have four GI-MMF categories specified in the generic cabling standards. Internationally, ISO/IEC 11801 specifies OM1, OM2, OM3, and OM4. For prevailing 10 Gigabit transmission speeds, OM3 is generally suitable for distances up to 300 m, and OM4 is suitable for distances up to 550 m. While OM3 and OM4 can support higher data rates and longer distances, there impact on installed base are not significant. Based on BSRIA (Building Services Research and Information Association) shipment data, the vast majority of commercial buildings and data centers are installed with OM1 and OM2 fibers. In order to use a common broadband in-house network infrastructure, in which a variety of services can be integrated, at low cost, we are interesting to exploit the existing OM1 and OM2 installations.

It is already known that the light propagates inside GI-MMFs in different modes, with each mode propagating at its respective group velocity [2]. The set of modes excited depends primarily on the launching of the light conditions at the input facet of the fiber [3]. To simultaneously transport various types of services having various bandwidths, the choice of any multiplexing technique depends on the high QoS and depends on the implementation cost of this technique. There exist several conventional techniques such wavelength-division multiplexing (WDM) based on the allocation of a wavelength to each service. However, this technique is limited by the capacity to generate adequate optical carrier. Indeed, WDM requires wavelength-specific sources in addition to wavelength-selective filter at the receiver, which are quite costly. Another candidate for multi-services systems called optical code-division multiple access (O-CDMA) that associate a sequence code to each service. However, spread spectrum with high flow rates (10 Gb/s) requires the use of lasers at high frequencies, which renders the system more expensive. MGDM is an O-MIMO technique that aims to create independent communication channels over MMF using subsets of propagating modes. It provides larger robustness and capacity for data communications and was introduced in order to improve the ability of a single MMF to integrate multi-services in a network [4]. As a result, new network appliances, such as telephones and televisions, will be added to the same data infrastructure. Already voice over Internet Protocol (VoIP) and Video on Demand (VoD) are being offered to consumers, over a single data network. The MGDM efficiently exploits fiber bandwidth by spatial launching and detection of the light; which increases the capacity of MMF [5]. We propose a new approach based on the optimization of the launching and detection conditions in order to increase the capacity of the O-MIMO link using MGDM technique. We propose a (3×3) O-MIMO system in order to improve GI-MMF capacity compared to existing O-MIMO systems.

This paper is organized as follows. In Section 2, the classical MGDM technique description details are given. In Section 3, we study methods on how to optimize transmission and detection conditions in order to increase channel capacity. Furthermore, a (3×3) MGDM system model is proposed and its performance details are explained. Simulation results showing the capacity improvement of our proposed system model as well a comparison with published research results are provided in Section 4. Finally, in Section 5, we draw conclusions from the obtained results.

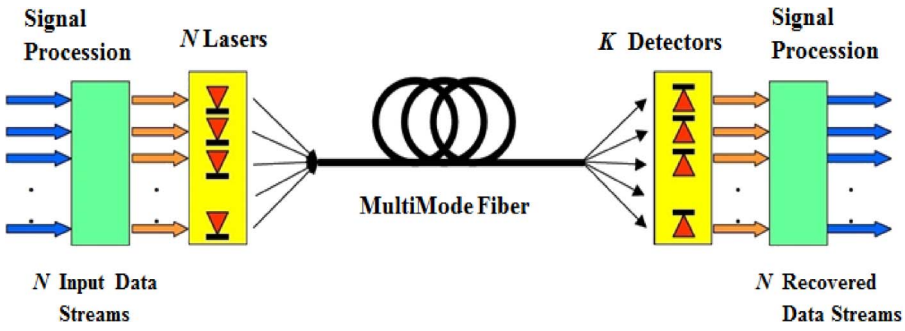

Fig. 1. Mode group diversity multiplexing principle.

2. Mode Group Diversity Multiplexing (MGDM)

Multiplexing in telecommunication systems allows several users to share the same transmission medium. The MGDM is a multiplexing technique model that enables parallel communication channels over a single MMF network. In this study, the MGDM has been proposed in order to integrate various services over a MMF network. The principle setup of MGDM is illustrated in Fig. 1.

At the transmitting side, N Lasers (light sources), each are used to launch a different group of modes. Modal interferences can be significantly minimized when different N sources of light are used for different mode groups. At the output facet of the MMF, a set of K photo-detectors respond to a different combination of the optical power carried by the N mode groups, related to the set of N lasers. The K received signals are related to the N transmitted signals via $(K \times N)$ the transmission matrix H, whose elements h_{ij} are the impulse responses of the ith output to the jth input.

The received signal (y) is expressed as follows:

$$y = H.s + n \tag{1}$$

where y, s, and n are the received signal vector, the emitted signal vector, and the additive noise from the receivers, respectively. Considering the hypothesis that H is known at the receiver, the capacity of the system is expressed as follows [6]:

$$C = B\log_2\left[\det\left(I_K + \frac{\rho}{N}HH^*\right)\right] \tag{2}$$

where B is the channel bandwidth, I_K is the unity $(K \times K)$ matrix, and ρ is the signal-to-noise ratio (SNR) at the input of the receiver array. The values of h_{ij} are given by [7]

$$h_{ij} = \frac{I_j(r_i, L)}{I_j(R, L)} \tag{3}$$

where I_j is the light flux intensity emitted by the jth transmitter, r_i is the area of the ith receiver, R is the total area of the core fiber, and L is the fiber length. The light flux intensity is given by

$$I(S,L) = \frac{1}{2}\sum_{\mu,\nu}\left|a_{\mu,\nu}(L)\right|^2 \int_S \Psi^2_{\mu,\nu}\,dS + \sum_{\mu\neq\mu'}\sum_{\nu\neq\nu'}\left[a_{\mu,\nu}(L)a_{\mu',\nu'}(L) \times \int_S \Psi_{\mu,\nu}\Psi_{\mu',\nu'}\,dS\right]\cos\left((\beta_{\mu,\nu} - \beta_{\mu',\nu'})L\right) \tag{4}$$

where $a_{\mu,\nu}$ and $\psi_{\mu,\nu}$ are the modal amplitude and the modal function of the (μ,ν) mode, respectively and $\beta_{\mu,\nu}$ is the light propagation constant. The parameters μ and ν are known as the radial

and azimuthal mode numbers, respectively. The determination of the intensity for each channel allows us to govern the coefficients of the matrix H which define the MGDM channel.

In order to calculate the intensity distribution at the end facet of the fiber, the values of the modal function $\psi_{\mu,\nu}$, the modal amplitude $a_{\mu,\nu}$ and the propagation0 constant $\beta_{\mu,\nu}$ should be determined. The modal function is given by the following expression:

$$\Psi_{\mu,\nu}(x,y) = \left(2^{\mu+\nu}\pi w_0 \mu!\nu!\right)^2 Hf_\mu\left(\frac{\sqrt{2}x}{w_0}\right) \times Hf_\nu\left(\frac{\sqrt{2}y}{w_0}\right).\exp\left(-\frac{x^2+y^2}{w_0^2}\right) \tag{5}$$

where w_0 is the spot size of the fundamental mode, and Hf is the Hermite function defined by:

$$H_p(x) = (-1)^p \exp(x^2)\frac{\partial^p}{\partial x^p}\exp(-x^2). \tag{6}$$

The modal amplitude is determined by the overlap integral given by the following equation:

$$a_{\mu,\nu}(z) = 2\left(\frac{w}{w_0}\right)\frac{1}{1+\left(\frac{w}{w_0}\right)^2}\left[\frac{w_0^2-w^2}{w_0^2+w^2}\right]^{\frac{\mu+\nu}{2}}\frac{1}{\sqrt{\mu!\nu!}}H_\mu\left(\frac{\sqrt{2}w_0F}{w_0^4-w^4}\right) \times H_\nu\left(\frac{k_0 n_0 \theta w_0 w^2}{2\left(w^4-w_0^4\right)}\right)\exp\left(-\frac{F^2}{w_0^2+w^2}-\frac{k_0^2 n_0^2 \theta^2 w_0^2 w^2}{4\left(w^4+w_0^4\right)}\right)\exp(-\gamma_{\mu,\nu}z) \tag{7}$$

where $\gamma_{\mu,\nu}$ is the attenuation coefficient of a MMF given by the following equation which has been proposed in [1] using experimental data from [8]:

$$\gamma_{\mu,\nu}(\lambda) = \gamma_0(\lambda)\left(1+\frac{\eta I_9}{M}[m-1]\right) \tag{8}$$

where γ_0 is the intrinsic attenuation of the fiber, I_9 is the 9th modified Bessel function, η is the weight constant, m is the principal mode number defined as $m = 2\mu+\nu+1$ and M is the total number of principal mode groups (PMGs). PMGs consist of modes with very similar propagation coefficient. The parameter m is a discrete integer which varies from 1 to M. In the approximation of low guidance, modes are combined into mode groups and propagate with the same modal propagation constant given by the following expression:

$$\beta_{\mu,\nu} = \sqrt{k_0^2 n_0^2 - \frac{2(2\mu+2\nu+2)}{w_0^2}} \tag{9}$$

where n_0 is the refractive index coefficient of the fiber, and k_0 is the free space wave-vector. The incident field at the input side of the fiber along the axis O_z, is considered as a Gaussian beam given by the following equation [9]:

$$E(x,y) = \frac{\sqrt{2}}{\sqrt{\pi w}}\exp\left(\left(-(x-F)^2-y^2\right)/w^2 - i\left(\frac{2n_0\pi\theta y}{\lambda}\right)\right) \tag{10}$$

where λ is the operating wavelength used in the transmission. F, w, and θ are the offset, the spot size, and the angular offset, respectively, which determine the excitation conditions of the MMF as illustrated below in Fig. 2. The field E is the superposition of the fields triggered by the sources (s_i).

3. Optimization of Excitation Conditions and Detection Parameters

The employment of the MGDM system in terms of capacity expansion gives rise to major interest in most current applications of optical communication systems. In this section, we study the

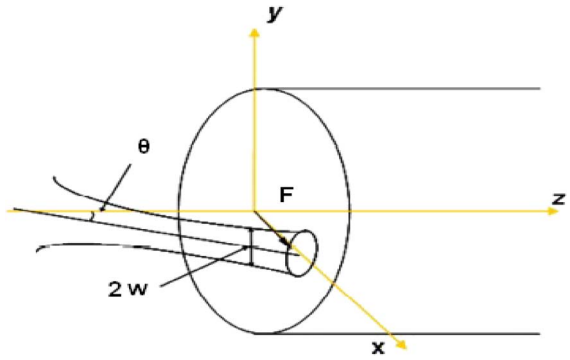

Fig. 2. Excitation geometry of the MMF by a Gaussian beam.

optimum selection criteria of transmitters and receivers in order to increase the capacity of the proposed optical communication system. The proposed model is a (3 × 3) MGDM system with optimal launching and detection parameters. Initially, we study the light flux intensity distribution. The distribution of the light flux intensity at the end facet of the fiber depends strongly on the number of excited modes in the input facet. The number of excited modes in the MGDM link depends mainly on the spatial excitation conditions (F, w, θ) and the wavelength λ, which have been carefully optimized in this study in order to help mitigate crosstalk in the MGDM link. The choice of the offsets is related to the optimization of the launching conditions in order to minimize the interference between the generated MIMO channels. In addition, for each launching offset, there is a specific region at the output facet of the fiber to collect the maximum light intensity at the receiver. The excitation of modes depends, not only on spatial conditions, but also on the used wavelength. In the following paragraphs, we present the optimization of the above key input/output parameters in order to select optimal conditions for the employed optical communication system.

3.1 Optimization and Selection of the Spot Size (w) and the Radial Offset (F)

The relationship between the spot size (w), the radial offset (F), and the total number of PMGs (M) is given by the following expression [10]:

$$M = \left(\frac{w_0}{w}\right)^2 + \begin{cases} \frac{4Fw}{w_0^2}, & \text{if } F > w \\ \frac{(F+w)^2}{w_0^2}, & \text{if } F < w. \end{cases} \tag{11}$$

The intensity distribution of the light at the output of the fiber depends on the number of excited modes at the input of the fiber. If, the number of excited modes is small, the intensity distribution is focused in a small radius. Changing the spot size or the radial offset of the incident beam at the input facet of the fiber affects the number of excited modes, and if at a given offset, the number of excited mode is small, the distribution of the light intensity power focuses on the fundamental modes. Otherwise, if the number of modes increases, the light intensity power of the fundamental modes decreases and the light intensity power of the end modes increases. For these reasons, the optimal spot size and the optimal radial offset correspond to the minimum value of M. Indeed, the distribution of the light intensity power is mainly focused on the fundamental modes.

3.2 Optimization and Selection of Angular Offset (θ)

For an incident light beam, there is only one optimal angle (θ) which has a maximum light intensity at the receiver output, corresponding to a minimum number of excited mode groups. The

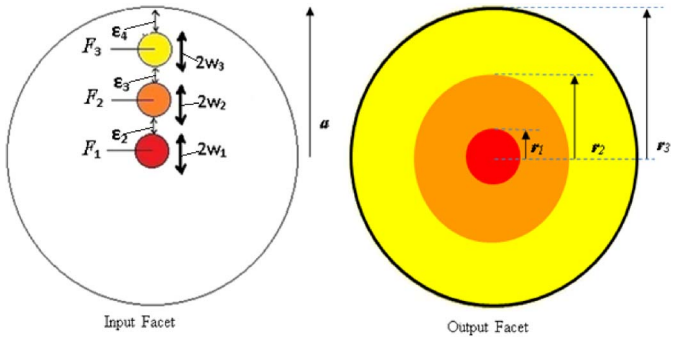

Fig. 3. Input and output facet of MMF for (3 × 3) MGDM system.

angular offset (θ) is related to the radial offset (F) and expressed by the equation [11]

$$\theta = \arcsin\left(\frac{F\ NA}{an_0\sqrt{1-2\Delta\left(\frac{F}{a}\right)^{\alpha}}}\right) \tag{12}$$

where a is the core radius of the MMF, α is the parameter that determines the shape of the profile in the fiber, and NA is the Numerical Aperture of the MMF.

3.3 Optimization and Selection of Wavelength (λ)

The excitation conditions of modes also depend on the wavelength (λ). The total mode group number of the MMF is related to the wavelength λ can be expressed as [12]

$$M = 2\pi a\frac{n_1}{\lambda}\sqrt{\frac{\alpha\Delta}{\alpha+2}}\,. \tag{13}$$

The optimum wavelength corresponds to the minimum of the excited mode group number. However, the modal attenuation of each spread mode of the fiber depends on the wavelength. It should be noted that modal attenuation of the signal generated by conventional loss mechanisms in the fiber such as absorption, Rayleigh scattering and reflection losses at the core-cladding interface have not been included in this study.

3.4 Analysis and Optimization of (3 × 3) MGDM Link

For the (3 × 3) MGDM link, three separate channels are generated in the GI-MMF by the injection of light in the three different offsets. The central transmitter launches only the lower-order modes, the two other transmitters launch higher-order modes which are mainly propagating in the outer region of the MMF core. At the reception (detection), every subgroup of modes has a specific area of optical energy distribution at the output facet of the fiber. The segment areas are chosen to minimize, on average, the optical cross-talk at the detector segments. Fig. 3 represents the input and the output facet of MMF for the (3 × 3) MGDM system, where F_i, w_i, $\varepsilon_{(i+1)}$ and r_i, $I = 1, 2, 3$ represents the radial offsets, the spot sizes, the spot light distances and the segments areas radius, respectively, of the detector relative to channel n° : i.

Optimal spot sizes (w_1, w_2, w_3) and radial offsets (F_1, F_2, F_3) are chosen to minimize the mode group number. These six parameters also depend on the fiber type, the fiber length and the used wavelength. The excited mode group number given by equation (11) depends both on the spot size and the radial offset. The geometry of the fiber must be taken into consideration in order to permit a separation distance (ε_2 and ε_3) between spot light sources. In these simulations, we have used the following two types of fibers (GI-MMF 62.5/125 μm "OM1"and GI-MMF

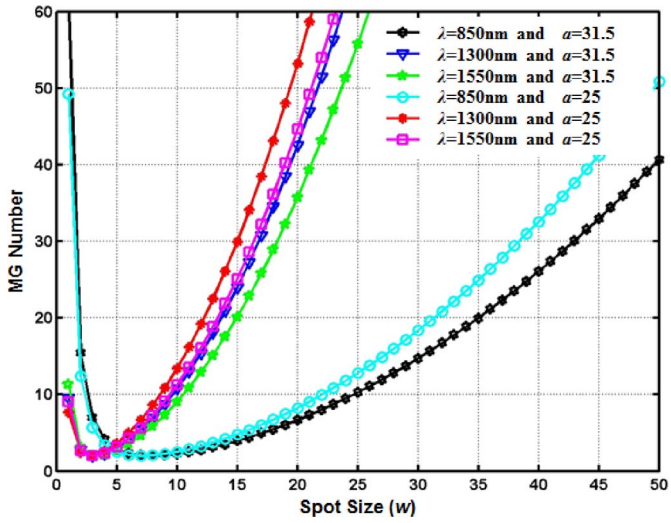

Fig. 4. The evolution of the excited mode group number distribution with the spot size for different wavelengths and two types of fibers (for first transmitter).

50/125 μm "OM2") with a length of 100 m, at different wavelengths ($\lambda = 850$ nm, 1300 nm, and 1550 nm).

The value of the first spot size w_1 must be smaller than the fiber radius a, and larger than a minimal value ε_1, presenting the smallest radius of the light beam source which can be used for the injection

$$\varepsilon_1 \leq w_1 \leq a. \tag{14}$$

The value of the first radial offset F_1 must be smaller than the fiber radius

$$0 \leq F_1 \leq a. \tag{15}$$

The calculated results for these parameters, using the equations (11)–(13), for the case when we use GI-MMF (50/125 μm), provide two possible injection conditions: First one is when $w_1 = 7$ μm, $F_1 = 0$ μm for wavelength $\lambda_1 = 850$ nm, and a second one when $w_1 = 3$ μm, $F_1 = 0$ μm for wavelength $\lambda_1 = 1550$ nm. For the case of when we use GI-MMF (62.5/125 μm), there are two possible injection conditions; the first one is when $w_1 = 3$ μm, $F_1 = 0$ μm for wavelength $\lambda_1 = 1550$ nm, and a second one is when $w_1 = 8$ μm, $F_1 = 0$ μm for wavelength $\lambda_1 = 850$ nm. This choice diversity of these optimal parameters is highly convenient for the user as it allows for more flexibility.

Fig. 4 shows the evolution of the excited mode group number for two types of fibers used in the system as a function of the spot size for different wavelengths. On the other hand, Fig. 5 shows the variation of the mode group number as a function of the radial offset for the first transmitter.

After we obtained these results, we then looked for the second injection parameters which provide the optimal excitation. The second beam light is physically constrained to have a minimum distance ε_2 from the first one to allow a separation distance of the two beam light sources. These physical constraints can be expressed by

$$\begin{aligned} &\varepsilon_1 \leq 2w_2 \leq a - w_1 - \varepsilon_2 \\ &w_1 + \varepsilon_2 \leq F_2 \leq a. \end{aligned} \tag{16}$$

The calculated results for these parameters for the GI-MMF (50/125 μm) provide optimal injection for $w_2 = 4$ μm and $F_2 = 17$ μm, at the wavelength $\lambda_2 = 850$ nm. While for the case of when

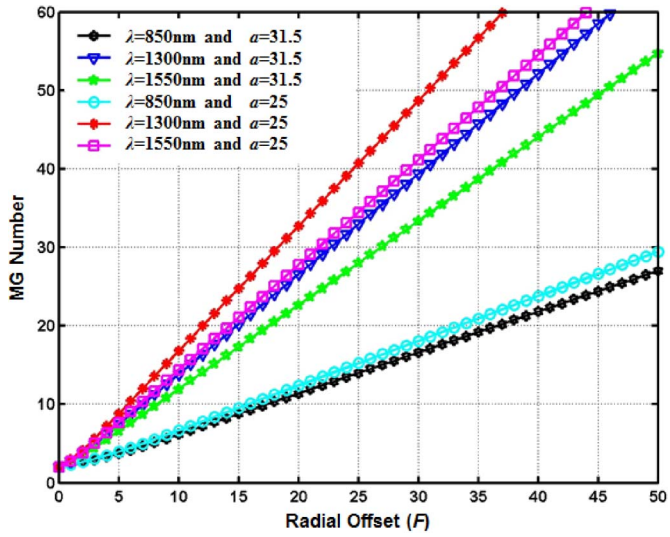

Fig. 5. The evolution of the excited mode group number distribution with the radial offset for different wavelengths and two types of fibers (for first transmitter).

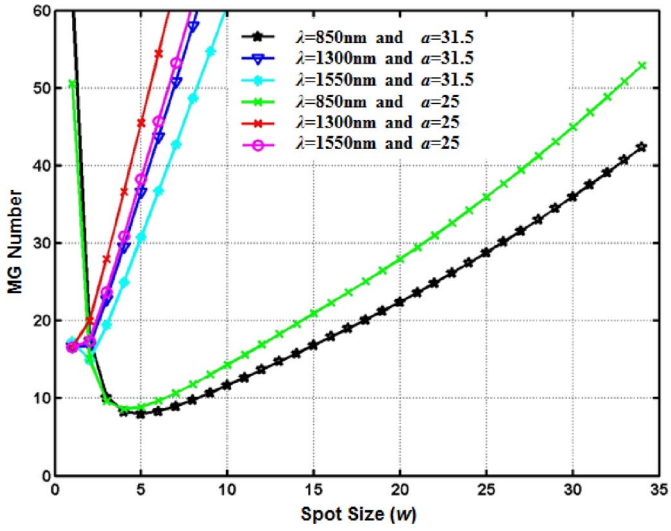

Fig. 6. The evolution of the excited mode group number distribution with the spot size for different wavelengths.

GI-MMF (62.5/125 μm), a possible optimal injection is obtained for $w_2 = 5$ μm, $F_2 = 17$ μm at the wavelength $\lambda_2 = 850$ nm.

Figs. 6 and 7 show the evolution of the excited mode group number with the spot size and the radial offset, respectively, for the second transmitter. For the third parameters, the physical constraints can be expressed by

$$\begin{aligned} &\varepsilon_1 \leq 2w_3 \leq a - w_1 - 2w_2 - \varepsilon_2 - \varepsilon_3 \\ &F_2 + w_2 + \varepsilon_3 \leq F_3 \leq a \end{aligned} \tag{17}$$

where ε_3 is the minimum distance between the second and third beam light sources. The third spot size must have a minimum distance separation ε_4 from the cladding of the fiber. The calculated results of third parameters for the GI-MMF (50/125 μm) gives the injection for $w_3 = 4$ μm,

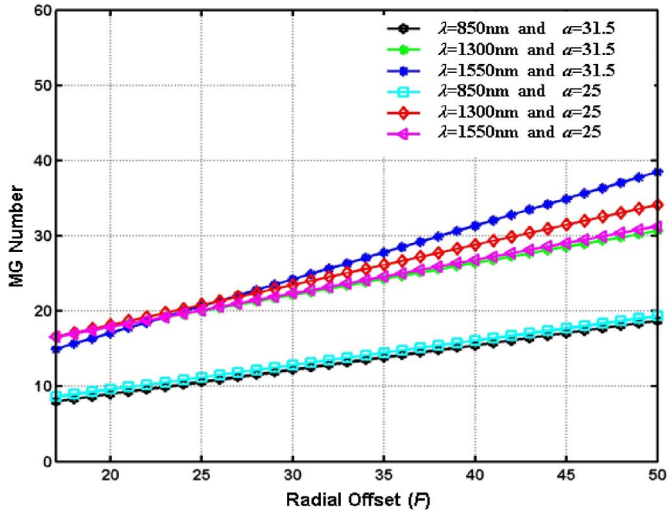

Fig. 7. The evolution of the excited mode group number distribution with the radial offset for different wavelengths and two types of fibers (for second transmitter).

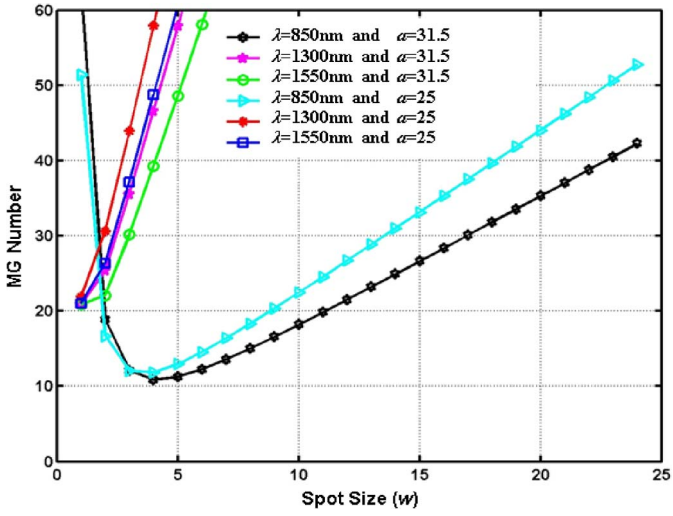

Fig. 8. The evolution of the excited mode group number distribution with the spot size for different wavelengths and two types of fiber (for third transmitter).

$F_3 = 27$ μm at wavelength $\lambda_3 = 850$ nm. For the case when the GI-MMF (62.5/125 μm) is used, a possible optimal injection is obtained for $w_3 = 4$ μm, $F_3 = 27$ μm at a wavelength of $\lambda_3 = 850$ nm.

Figs. 8 and 9 show the evolution of the excited mode group number as a function of the spot size and the radial offset for the third transmitter. Calculations of the results have been performed using equation (12), where the optimal angular offset is $\theta_1 = 0^\circ$, $\theta_2 = 3.6442^\circ$, and $\theta_3 = 5.818^\circ$ for the case when GI-MMF (50/125 μm) is used. The angular offsets θ_1, θ_2, and θ_3 are associated with the first, second, and third transmitter, respectively, whereas for the case when GI-MMF (62.5/125 μm) is used, the calculated results are as follows: $\theta_1 = 0^\circ$, $\theta_2 = 2.9126^\circ$, and $\theta_3 = 4.638^\circ$.

If we refer to Fig. 3, we can see that the output facet of the fiber is divided into three circular sections corresponding to three different injections. Every subgroup of modes has a specific area of detection. For the first transmitter, light energy is concentrated into the middle of the

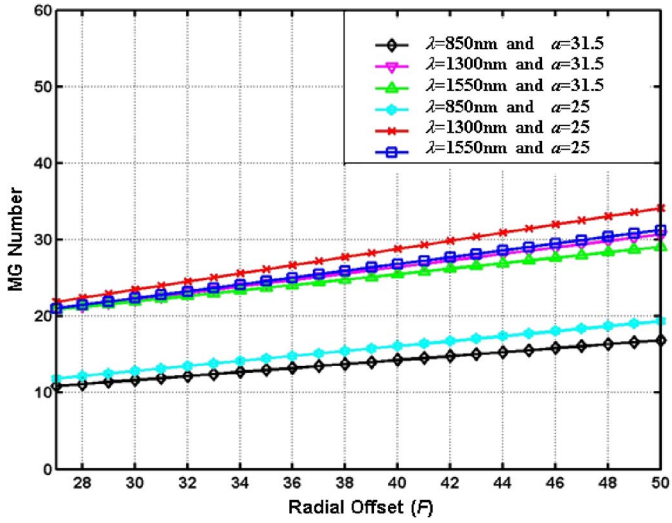

Fig. 9. The evolution of the excited mode group number distribution with the radial offset for different wavelengths and two types of fiber (for third transmitter).

fiber core zone. It should be noted that the lowest mode will carry more energy. However, the light energy of the two other transmitters is distributed in the outside region of the core as a result of the higher order modes being excited.

In order to increase the orthogonality between channels and consequently increase the capacity of the system, the optimal receivers are chosen by determining the maximum intensity of light flux in each detection area of the corresponding transmitter.

For the fundamental channel ($F_1 = 0\ \mu$m), the optimal reception area of light energy is concentrated in the middle of the fiber core with a radius R_1 ($R_1 = r_1$). The optimal detection area corresponding to the second injection is concentrated in the zone of radius R_2 ($r_1 < R_2 < r_2$). For the third transmitter, the optimal detection area is concentrated in the zone of radius R_3 ($r_2 < R_3 < a$).

The calculated results of optimal reception parameters for GI-MMF (50/125 μm) with injection conditions: w1 $= 3\ \mu$m, F1 $= 0\ \mu$m, w2 $= 4\ \mu$m, F2 $= 17\ \mu$m, w3 $= 4\ \mu$m, and F3 $= 27\ \mu$m, gives r1 $= 8\ \mu$m and r2 $= 23\ \mu$m. For the same kind of fiber with injection conditions: w1 $= 7\ \mu$m, F1 $= 0\ \mu$m, w2 $= 4\ \mu$m, F2 $= 17\ \mu$m, w3 $= 4\ \mu$m, and F3 $= 27\ \mu$m, the calculated results gives r1 $= 10\ \mu$m and r2 $= 23\ \mu$m. For the case of a GI-MMF (62.5/125 μm) with injection conditions w1 $= 3\ \mu$m, F1 $= 0\ \mu$m, w2 $= 5\ \mu$m, F2 $= 17\ \mu$m, w3 $= 4\ \mu$m, and F3 $= 27\ \mu$m the calculated results gives r1 $= 7\ \mu$m and r2 $= 23\ \mu$m. For the same kind of fiber with injection conditions w1 $= 8\ \mu$m, F1 $= 0\ \mu$m, w2 $= 5\ \mu$m, F2 $= 17\ \mu$m, w3 $= 4\ \mu$m, and F3 $= 27\ \mu$m, the calculated results gives r1 $= 11\ \mu$m and r2 $= 23\ \mu$m.

The choice of excitation and reception settings can be summarized by the diagram shown in Fig. 10. This diagram describes the calculating steps of the optimal transmission and reception conditions.

3.5 Proposed Model

We propose a (3 $\times$ 3) MGDM system, as illustrated in Fig. 11. It should be noted that the MMF is presented as a multipath channel. The three received signals are directly related to the three transmitted signals via (3 $\times$ 3) transmission matrix H, whose elements are h_{ij}, $i, j = 1, 2, 3$, as defined by the equation (3). The (3 $\times$ 3) MGDM model employs the optimized transmitters and receivers.

The calculated results of the optimal injection and detection parameters for the two types of fibers employed in this proposed optical system model are presented in Table 1.

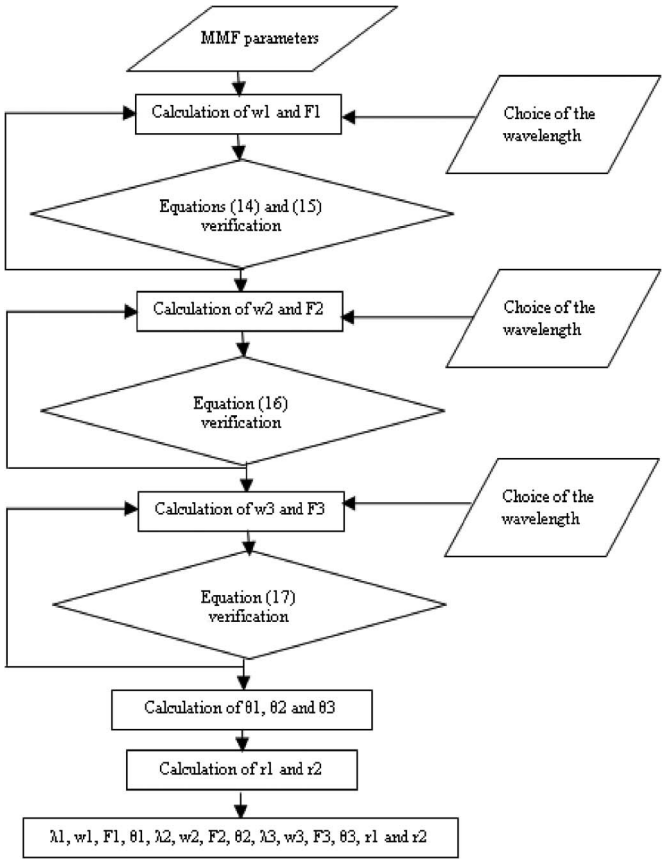

Fig. 10. Optimization diagram.

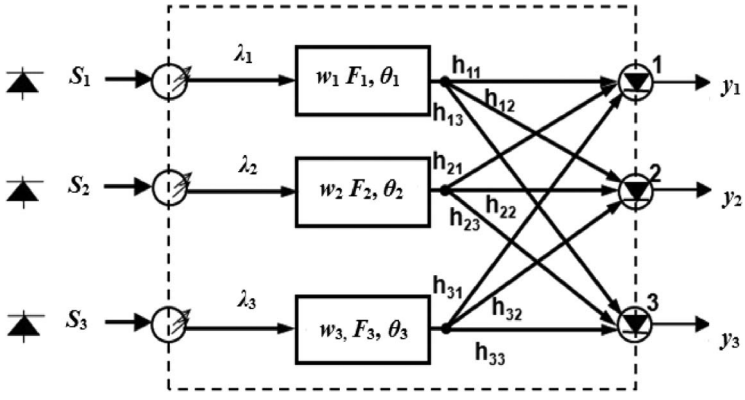

Fig. 11. Proposed (3 × 3) MGDM Model.

4. Simulation Results

MGDM is known to improve the network capacity, and it enables the integration of different services in a network, allowing the optimal use of the optical bandwidth. Parameters of injection and reception are the principal elements of the MGDM technique realization. These characteristics influence the system capacity and the quality of the transmission. For these reasons and to evaluate our system performance, we will calculate its capacity. Moreover, we will compare the simulation results of our system to other research results.

TABLE 1

Optimal injection and reception parameters

Fiber Type	Optimal injection parameters	Optimal reception parameters
GI-MMF (50/125μm)	λ_1=1550nm w_1=3μm F_1=0μm θ_1=0° λ_2=850nm w_2=4μm F_2=17μm θ_2=3.6442° λ_3=850nm w_3=4μm F_3=27μm θ_3=5.818°	r_1=8μm r_2=23μm
	λ_1=850nm w_1=7μm F_1=0μm θ_1=0° λ_2=850nm w_2=4μm F_2=17μm θ_2=3.6442° λ_3=850nm w_3=4μm F_3=27μm θ_3=5.818°	r_1=10μm r_2=23μm
GI-MMF (62.5/125μm)	λ_1=1550nm w_1=3μm F_1=0μm θ_1=0° λ_2=850nm w_2=5μm F_2=17μm θ_2=2.9126° λ_3=850nm w_3=4μm F_3=27μm θ_3=4.638°	r_1=7μm r_2=23μm
	λ_1=850nm w_1=8μm F_1=0μm θ_1=0° λ_2=850nm w_2=5μm F_2=17μm θ_2=2.9126° λ_3=850nm w_3=4μm F_3=27μm θ_3=4.638°	r_1=11μm r_2=23μm

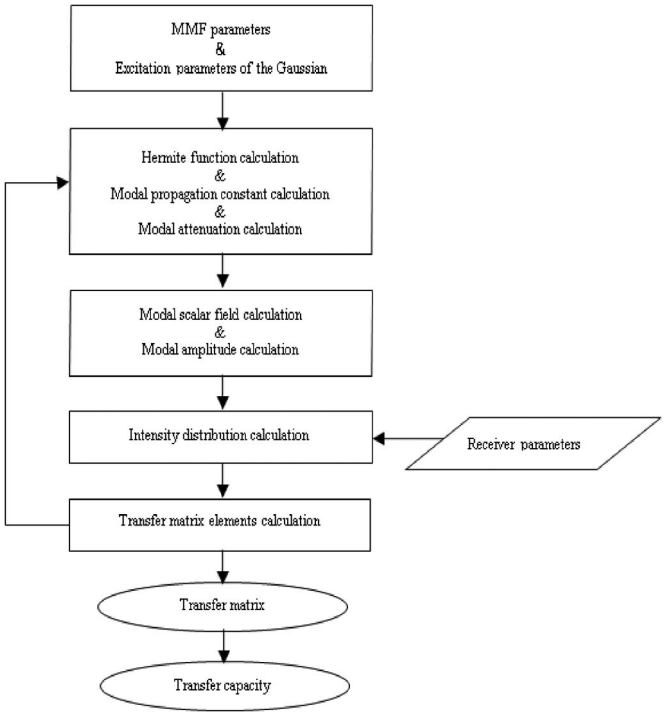

Fig. 12. Calculating algorithm of the transfer matrix and the channel capacity.

4.1 Calculating Algorithm of the Transfer Matrix and the Channel Capacity

In this section, we propose our algorithm to calculate the transfer matrix "H" and the system capacity "C," of our MGDM link. This algorithm is illustrated in Fig. 12.

In this algorithm, we start by initializing the program data. These data are the used MMF parameters (length, refractive indices, etc.) and the launching conditions (spot sizes, radial offsets, angular offsets, wavelengths, etc.). Next, we calculate the Hermite function, the modal propagation constant and the modal attenuation by varying the radial and the azimuthal mode numbers using the relationship which reads these numbers to the mode number. After that, we calculate the modal scalar field and the modal amplitude. Knowing the receiver parameters, we calculate subsequently the light intensity distribution caused by each transmitter. This step is repeated for

TABLE 2

Injection and reception parameters in [12]

Fiber Type	Optimal injection parameters	Optimal reception parameters
GI-MMF (50/125μm)	F_1=0μm, F_2=13μm, F_3=26μm $w_1 = w_2 = w_3 = w = 4\mu m$ $\theta_1 = \theta_2 = \theta_3 = 0°$ $\lambda_1 = \lambda_2 = \lambda_3 = 850nm$	$r_1 = 7\mu m, r_2 = 16\mu m$
GI-MMF (62.5/125μm)	F_1=0μm, F_2=13μm, F_3=26μm $w_1 = w_2 = w_3 = w = 4\mu m$ $\theta_1 = \theta_2 = \theta_3 = 0°$ $\lambda_1 = \lambda_2 = \lambda_3 = 850nm$	$r_1 = 7\mu m, r_2 = 16\mu m$

all different transmitters and receivers combinations. The total intensity distribution is the sum of the intensity distribution of the light flux generated by the various transmitters. The proportion value of the received power at the output facet of the fiber of each mode group allows us to find the elements of the transfer matrix. When the matrix is determined, it becomes easy to calculate the system capacity.

4.2 Results and Discussion

For the case of the GI-MMF (50/125 μm) fiber with the following injection parameters: $\lambda_1 = 850$ nm, $w_1 = 7\ \mu$m, $F_1 = 0\ \mu$m, $\theta_1 = 0°$, $\lambda_2 = 850$ nm, $w_2 = 4\ \mu$m, $F_2 = 17\ \mu$m, $\theta_2 = 3.6442°$, $\lambda_3 = 850$ nm, $w_3 = 4\ \mu$m, $F_3 = 27\ \mu$m, $\theta_3 = 5.818°$, and the reception conditions $r_1 = 10\ \mu$m and $r_2 = 23\ \mu$m, the calculated results of the matrix H defined by (3) are as follows:

$$H = \begin{pmatrix} 0.8200 & 0.0845 & 0.0752 \\ 0.1708 & 0.8290 & 0.2050 \\ 0.0092 & 0.0856 & 0.7198 \end{pmatrix}.$$

For the case of the GI-MMF (62.5/125 μm) fiber with the following injection parameters: $\lambda_1 = 850$ nm, $w_1 = 8\ \mu$m, $F_1 = 0\ \mu$m, $\theta_1 = 0°$, $\lambda_2 = 850$ nm, $w_2 = 5\ \mu$m, $F_2 = 17\ \mu$m, $\theta 2 = 2.9126°$, $\lambda_3 = 850$ nm, $w_3 = 4\ \mu$m, $F_3 = 27\ \mu$m, $\theta_3 = 4.638°$, and the following reception conditions $r_1 = 11\ \mu$m and $r_2 = 23\ \mu$m, calculated results of the matrix H are

$$H = \begin{pmatrix} 0.9120 & 0.1153 & 0.0641 \\ 0.0874 & 0.8765 & 0.1921 \\ 0.0006 & 0.0082 & 0.7438 \end{pmatrix}.$$

In this case, we evaluate the capacity of the proposed system given by equation (2) and then we compare the simulated results with those published by Awad *et al.* [13], where the launching and reception parameters are shown in Table 2.

Figs. 13 and 14 show the capacity improvement obtained by using our proposed emitter for the following fibers: GI-MMF (62.5/125 μm) and GI-MMF (50/125 μm).

Figs. 13 and 14 illustrate the capacity of the MMF as a function of SNR for single-input–single-output (SISO), (3 $\times$ 3) MGDM reported in [12], and our proposed (3 $\times$ 3) MGDM model. It is clear to see that our proposed optical system model, for two the types of MMF, shows significantly increased capacity performance compared to the reported results in [12]. The capacity, in the case of MGDM (3 $\times$ 3), under the optimal conditions increases rapidly when the SNRs is increased. An average gain of 8 bits/s/Hz and 26 bits/s/Hz is obtained compared to [12] and the SISO system, respectively, when SNR $=$ 30 dB.

For low SNRs, our system shows a capacity gain around 2 bits/s/Hz at SNR $=$ 5 dB for the case when the GI-MMF (62.5/125 μm) fiber is used, and around 1 bits/s/Hz at the same SNR

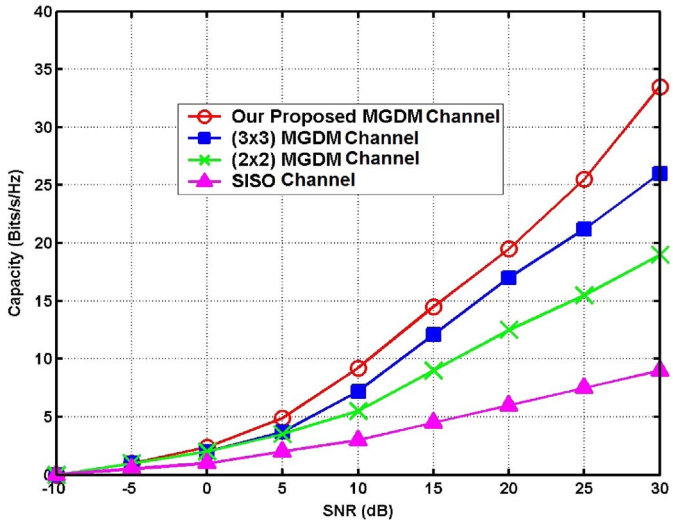

Fig. 13. GI-MMF (62.5/125 μm) capacity as a function of SNR.

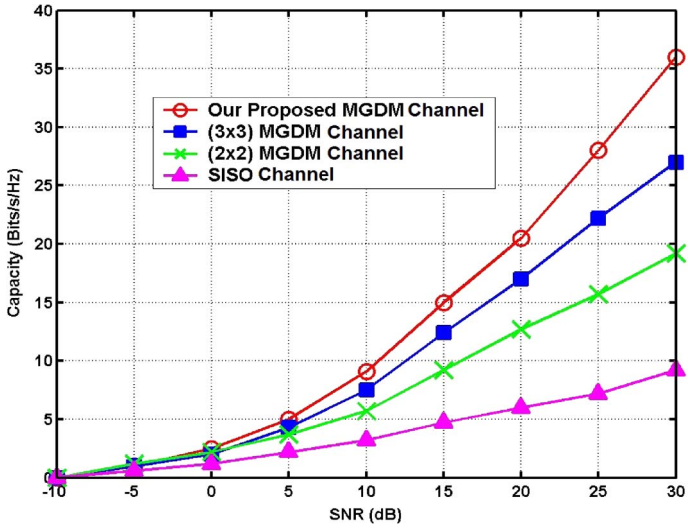

Fig. 14. GI-MMF (50/125 μm) capacity as a function of SNR.

for the case when the GI-MMF (50/125 μm) is used, in comparison to [12]. We can also quite evidently see an improvement in the capacity gain of 3 bits/s/Hz compared to the SISO channel at the same SNR for the two types of the fibers used in the system.

From Fig. 14, it can be seen that capacity increases as a function of the SNR and in particular, a major increase can be noted when our proposed optimized system is deployed compared to (3 $\times$ 3) MGMDM, (2 $\times$ 2) MGMDM, and SISO.

5. Conclusion

In this paper, an analytical study and optimization of MGDM link is presented. The impact of injection and reception conditions in order to improve the capacity of multimode fibers is demonstrated for a (3 $\times$ 3) MGDM proposed optical system. The excited mode group number is used as a matrix to determine the optimum radial and angular offsets, spot size, and wavelengths. Optimization of the key launching and detection parameters of the proposed optical system for

three transmitters is demonstrated. The efficiency of the proposed optimized optical MIMO is reported in rigorous manner signifying improvements when compared to current MGDM systems. In our future work, we will take into account the conventional loss mechanisms.

References

[1] G. Yabre, "Comprehensive theory of dispersion in graded-index optical fibers," *J. Lightw. Technol.*, vol. 12, no. 2, pp. 166–176, Feb. 2000.

[2] D. M. Kuchta *et al.*, "120-Gb/s VCSEL based parallel optical interconnect and custom 120-Gb/s testing station," *J. Lightw. Technol.*, vol. 22, no. 9, pp. 2200–2212, Sep. 2004.

[3] S. Haxha, O. L. Emmanuel, M. Mjeku, F. AbdelMalek, and B. M. A. Rahman, "Optimization of compact lateral, vertical, and combined spot-size converters by use of the beam propagation method," *J. Appl. Opt.*, vol. 45, no. 2, pp. 288–296, Jan. 2006.

[4] T. Koonen, H. P. A. Van den Boom, I. T. Monroy, and G.-D. Khoe, "High capacity multi-service in house networks using mode group diversity multiplexing," presented at the Opt. Fiber Commun. Conf., Los Angeles, CA, USA, 2004, Paper FG4.

[5] T. Koonen, H. Van den Boom, F. Willems, J. Bergmans, and G.-D. Khoe, "Broadband multi-service in house networks using mode group diversity multiplexing," in *Proc. Int. Plastic Opt. Fibers Conf.*, Tokyo, Japan, 2002, pp. 87–90.

[6] E. Telatar, "Capacity of multi-antenna Gaussian channels," *Eur. Trans. Telecommun.*, vol. 10, no. 6, pp. 585–595, Nov./Dec. 1999.

[7] M. Awad, I. Dayoub, W. Hamouda, and J. M. Rouvaen, "Adaptation of the mode group diversity multiplexing technique for radio signal transmission over MMF," *IEEE/OSA J. Opt. Commun. Netw.*, vol. 3, no. 1, pp. 1–9, Dec. 2011.

[8] M. Rousseau and L. Jeunhomme, "Optimum index profile in multimode optical fiber with respect to mode coupling," *Opt. Commun.*, vol. 23, no. 2, pp. 275–278, Nov. 1977.

[9] A. R. Shah, R. S. J. Hsu, A. Tarighat, A. H. Sayed, and B. Jalali, "Coherent optical MIMO (COMIMO)," *J. Lightw. Technol.*, vol. 23, no. 8, pp. 2410–2419, Aug. 2005.

[10] L. Raddatz, I. H. White, D. G. Cunningham, and M. C. Nowell, "An experimental and theoretical study of the offset launch technique for the enhancement of the bandwidth of multimode fiber links," *J. Lightw. Technol.*, vol. 16, no. 3, pp. 324–331, Mar. 1998.

[11] M. Calzavara, R. Caponi, and F. Cisternino, "Selective excitation of annular zones in graded index multimode fiber," *J. Opt. Commun.*, vol. 5, no. 3, pp. 82–86, 1984.

[12] P. Hillion, "Electromagnetic pulse propagation in dispersive media," *Progr. Electromagn. Res.*, vol. 35, 299–314, 2002.

[13] M. Awad, I. Dayoub, O. Okassa-M'foubat, and J.-M. Rouvaen, "The inter-modes mixing effects in mode Group diversity multiplexing," *Opt. Commun.*, vol. 282, no. 19, pp. 3908–3917, Oct. 2009.